Risk Assessment Method for Distributed Power Distribution Networks Considering Network Dynamic Reconstruction

Tangyong Teng[1], Yu Huang[1,*], Juan Wang[2], Zhukun Li[2], Yonghua Chen[2]
[1]Institute of Advanced Technology for Carbon Neutrality, Nanjing University of Posts and Telecommunications, Wenyuan St. 9, Nanjing, China
[2]NARI Technology Co., Ltd., Chengxin St. 19, Nanjing, China
1760617382@qq.com; [*]huang_hy_hy@126.com; wangjuan5@sgepri.sgcc.com.cn; lizhukun@sgepri.sgcc.com.cn; chenyonghua@sgepri.sgcc.com.cn

***Abstract*—A new safety assessment framework has been proposed to address the operational risks of the integration of wind power and photovoltaic grid, which integrates the characteristics of distributed power sources with the dynamic reconfiguration requirements of the distribution grid. The framework comprehensively considers the impacts of wind power and photovoltaic output uncertainties, as well as load fluctuations, on the stability of the distribution grid. It also evaluates the safety under different operational states of the distribution grid. Using Halton sequence sampling technology to accurately simulate the output of distributed power sources and the status of system components, combined with CPLEX optimisation for solving, a dynamic reconfiguration model is constructed to address potential faults in the distribution grid. Introducing the combined weighting method, a comprehensive risk assessment system for voltage violations, power flow violations, and load shedding has been constructed. The effectiveness of this method has been validated through simulations on the IEEE33 bus and IEEE118 bus systems, providing new insights to improve the safety and reliability of distribution grids.**

***Index Terms*—Stochastic power flow; Distribution network reconfiguration; Combination weighting; Risk assessment.**

I. INTRODUCTION

A. Motivations

With the deepening implementation of China's "dual carbon" strategic goals, the installed capacity of new energy continues to increase steadily, especially wind power and photovoltaic power generation, which play an increasingly important role in the transformation of the energy structure as crucial components of clean energy. However, with the wide access of the distributed power supply, its uncertainty poses challenges to the stable operation of the distribution network. To cope with the actual situation, the distribution network risk assessment needs not only to have an accurate prediction of the distributed output, but also to take into account the reliability of the system operation to ensure that possible failures are effectively dealt with and to calculate the risk in different situations. Therefore, a safety evaluation method is urgently needed to combine accuracy and reliability to ensure the safe operation of the distribution network.

In the field of safety assessment for distribution networks, one of the primary challenges currently faced is how to accurately quantify distributed power sources, especially the impact brought about by the integration of wind power and photovoltaic power generation. Random power flow analysis, as a core quantitative analysis tool, revolves around models for output prediction of distributed power sources, methods for calculating random power flow, and indicators and methods of safety assessment. In [1], a solar irradiance probability density model is established targeting the volatility of photovoltaic output by combining adaptive kernel density estimation with the Cornish-Fisher expansion method, thus improving the accuracy of photovoltaic output prediction. In [2], employing the Copula theory and Cholesky decomposition method, an in-depth analysis of the correlation between wind power and photovoltaic output is carried out, thus optimising the input parameters of random power flow analysis and improving the accuracy of the calculation. Furthermore, nonparametric kernel density estimation is applied in [3] to establish a photovoltaic probability model, further refining the accuracy of output prediction. Simultaneously, the state model and the wind power output prediction error model proposed in [4] based on state-space methodology provide a new perspective for understanding the dynamic characteristics of wind power and prediction errors. From the perspective of the prediction model, the above work improves the accuracy of distributed power supply prediction and lays a foundation for the accuracy of risk assessment.

At present, a lot of achievements have been made in the construction of distribution network risk assessment system and methods. In [5], based on risk value theory, taking load shedding and voltage violation as indicators, a hierarchical risk assessment system is designed that provides a new quantitative assessment method for the distribution network. In [6], a specific risk assessment system is established from

Manuscript received 17 March, 2024; accepted 12 June, 2024.
This research was supported by the Natural Science Foundation of Jiangsu Province under Grant No. BK20232026; China Postdoctoral Science Foundation under Grant No. 2023M741801.

the perspective of voltage violation and load shedding caused by harmonic distortion. In [7], based on domestic and foreign distribution network reliability indicators combined with risk assessment indicators, a new safety assessment system is constructed for the distribution network. The above works use different indicators for evaluation, but they all remain at the level of static evaluation, only assessing the risk of a specific state without considering the reliability of the distribution network operation, lacking consideration of actual situations. In [8], it is emphasised that the safety assessment of the distribution network should be distinguished from the characteristics of the power system, and the authors propose a static risk assessment method suitable for the characteristics of the distribution network based on risk theory and the K(N - 1 + 1) criterion. Although the reliability of system operation is considered, the work still lacks a comprehensive analysis of all possible fault scenarios that may occur in actual scenarios.

Although the above research provides a series of theoretical methods, including prediction and evaluation for assessing the security of the distribution network, the operation of the system in practical applications is not static, and the reliability of the power supply of the distribution network should be considered comprehensively, especially the in-depth analysis of the status of the equipment and the operation status of the system. How to incorporate reliability into the risk assessment process while taking into account accuracy and reliability is still a key problem to be solved. Future demands for energy supply will increasingly emphasise flexibility, safety, and security [9].

B. Contributions

To overcome the above problems, this paper proposes a method of assessing the risk of the distribution network considering network reconstruction and attempts to integrate the consideration of system operation reliability into the risk assessment process. Contributions are as follows.

– Different from the typical static risk assessment of the distribution network, which does not consider component failure, this paper not only establishes the model of distributed power supply, but also considers the reliability of system components. The traditional static risk assessment is transformed into dynamic risk assessment by introducing a distribution network reconstruction model and anticipating system failure to recover. The problem of how to combine forecast accuracy with operational reliability for risk assessment is solved.

– To address the issue of large sampling scales, the Halton sequence sampling method is used instead of the Monte Carlo method, reducing the number of sample samples and improving the efficiency of evaluation.

– By selecting three evaluation indexes of voltage, power flow, and load loss, the analytic hierarchy process and entropy weight method are combined to solve the shortcomings of single evaluation method and make the distribution network risk assessment results more objective and reasonable. The influence of the location and capacity of the distributed power supply on the risk value of the distribution network is analysed.

This paper is organised as follows. Short-term wind power, photovoltaic, and load models, as well as short-term system component state models, are constructed, and samples are generated using the Halton sequence sampling method in Section II. We constructed a distribution network reconstruction model in Section III. Indicators and evaluation methods for risk assessment are introduced in Section IV. Section V presents the results of the test cases, with conclusions placed in Section VI.

II. DISTRIBUTION NETWORK RANDOM POWER FLOW WITH DISTRIBUTED GENERATION

A. Distributed Generation Model

Wind speed determines the output of wind turbines, which is generally simulated using the Weibull distribution. The probability density function of wind speed is as follows

$$f(v)=\frac{k}{c}(\frac{v}{c})^{k-1}\exp[-(\frac{v}{c})^{k}], \tag{1}$$

where v is the wind speed (m/s), k is the shape parameter, and c is the scale parameter.

The relationship between wind turbine output power and wind speed is as follows [10]

$$P_{wt}(v)=\begin{cases}0, & v<v_{ci}, v>v_{co},\\ \dfrac{P_r(v-v_{ci})}{(v_r-v_{ci})}, & v_{ci}<v<v_r,\\ P_r, & v_r<v<v_{co},\end{cases} \tag{2}$$

where P_{wt} stands for the output active power output, v represents the real-time wind speed, v_{ci} represents the cut-in wind speed of the fan, v_{co} represents the cut-out wind speed of the fan, v_r indicates the rated wind speed of the fan, P_r indicates the rated power of the fan.

Generally, the output of photovoltaic systems is simulated using the Beta distribution [11]:

$$f(r)=\frac{\Gamma(\alpha+\beta)}{\Gamma(\alpha)+\Gamma(\beta)}(\frac{r}{r_{\max}})^{\alpha-1}(1-\frac{r}{r_{\max}})^{\beta}, \tag{3}$$

$$P_{pv}=rA\eta, \tag{4}$$

where α and β are the parameters of Beta distribution, r is the actual value of solar illumination intensity at a certain time in the short term, $r_{\max}$ is the maximum light intensity in the short term, η is the conversion efficiency of photovoltaic to electric energy, $\Gamma(\cdot)$ is the gamma function, A stands for the area, $f(r)$ is the probability density function of light intensity, and P_{pv} is photovoltaic active power output.

Due to the inherent variability and uncertainty of the loads, it is generally assumed that they follow a normal distribution [12]:

$$f(P)=\frac{1}{\sqrt{2\pi}\sigma_p}\exp[-\frac{(P-\mu_p)^2}{2\sigma_p^2}], \tag{5}$$

$$f(Q)=\frac{1}{\sqrt{2\pi}\sigma_q}\exp[-\frac{(Q-\mu_q)^2}{2\sigma_q^2}], \tag{6}$$

where P is the active load, μ_p is the active expectation, σ_p is the active standard deviation, Q is the reactive load, μ_q is the reactive expectation, and σ_q is the reactive standard deviation.

B. System Fault State Model

Wind turbine forced outage rate and probability of wind turbine fault states [13]:

$$\begin{cases} r_{wt} = \dfrac{\lambda_{wt}}{\lambda_{wt} + \mu_{wt}}, \\ \mathrm{Pr}_{wt,t} = 1 - e^{-t \times r_{wt}}, \end{cases} \tag{7}$$

where λ_{wt} represents the failure rate of the wind turbine, μ_{wt} represents the repair rate of the wind turbine, $\mathrm{Pr}_{wt,t}$ is the failure probability of the fan, and r_{wt} is the forced outage rate of the fan.

Forced outage rate of photovoltaic modules and probability of photovoltaic failure states [14]:

$$\begin{cases} r_{pv} = \dfrac{\lambda_{pv}}{\lambda_{pv} + \mu_{pv}}, \\ \mathrm{Pr}_{pv,t} = 1 - e^{-t \times r_{pv}}, \end{cases} \tag{8}$$

where λ_{pv} indicates the failure rate of photovoltaic modules, μ_{pv} represents the repair rate of photovoltaic modules, $\mathrm{Pr}_{pv,t}$ indicates the fault probability of the photovoltaic, and r_{pv} represents the forced outage rate of the photovoltaic.

The probability of a line fault state is as follows [15]

$$\mathrm{Pr}_{l,i,t} = 1 - e^{-t \times r_{l,i}}, \tag{9}$$

where $r_{l,i}$ is the failure rate of the line and $\mathrm{Pr}_{l,i,t}$ indicates the fault probability of line.

C. Halton Sequence Sampling Method

To reduce computational complexity, efficient sampling of distributed output data and system component states is required. The Halton method is a numerical computation technique that utilises low-discrepancy sequences and falls under quasi-Monte Carlo methods. Monte Carlo methods are suitable for problems requiring a large number of samples, offering high flexibility but slow convergence; Halton sequence sampling is suitable for numerical computations in lower dimensions, providing faster convergence rates and more uniform distribution characteristics.

The general steps of Halton sequence sampling are as follows. First, choose different bases for each dimension, ensuring that they are coprime, such as 2, 7, etc. Then convert the generated indices into numbers represented in the chosen base and mirror-reverse them. Next, convert the reversed decimals into decimal numbers, which represent the sampling points for the current dimension. Finally, since the generated Halton sequence is in the range [0, 1], map it back to the original sampling space.

Using the Halton method to obtain samples of wind turbine, photovoltaic, and load data, as well as the states of system components, a significant reduction in the number of samples compared to MC is achieved.

III. Distribution Network Reconstruction

To facilitate fault recovery, in this section it is necessary to establish a distribution network reconstruction model.

A. Objective Function

This paper takes the minimum active power loss of the network as the objective function

$$\min P_{loss} = \sum_{ij \in E} I_{ij}^2 r_{ij}, \tag{10}$$

where P_{loss} is the sum of the active power loss of each branch of the distribution network, r_{ij} is the resistance of the branch, I_{ij} is the current of the branch, and E represents the set of branches.

B. Power Flow Constraint

Based on the Distflow power flow model, this paper deals with the problem of switching on and off by introducing the variable of branch on-off state [16]

$$\begin{cases} \sum\limits_{i \in f(j)} \alpha_{ij}(P_{ij} - r_{ij} I_{ij}^2) = \sum\limits_{k \in s(j)} \alpha_{jk} P_{jk} + P_j, \\ \sum\limits_{i \in f(j)} \alpha_{ij}(Q_{ij} - x_{ij} I_{ij}^2) = \sum\limits_{k \in s(j)} \alpha_{jk} Q_{jk} + Q_j, \\ P_j = P_j^{wind} + P_j^{pv} - P_j^{load}, \\ Q_j = Q_j^{wind} + Q_j^{pv} - Q_j^{load}, \\ U_j^2 = U_i^2 - 2(r_{ij} P_{ij} + x_{ij} Q_{ij}) + (r_{ij}^2 + x_{ij}^2) I_{ij}^2, \\ (U_i I_{ij})^2 = P_{ij}^2 + Q_{ij}^2, \end{cases} \tag{11}$$

where P_{ij} and Q_{ij} are the active and reactive power flowing on the branch, respectively, x_{ij} is the reactance of the branch, P_j and Q_j are the active and reactive power, respectively, P_j^{load} and Q_j^{load} are the active power load and reactive power load, respectively, P_j^{wind} and Q_j^{wind} are the wind power active and reactive power, P_j^{pv} and Q_j^{pv} are the photovoltaic active and reactive power, and $f(j)$ and $s(j)$ are the set of parent and child nodes.

Due to the fact that the constraints in (11) are only applicable to closed branches, inequality (12) is introduced to relax them. Consequently, the constraints in (11) can be applied to situations involving nonclosed branches. Furthermore, by introducing equivalent variables U_i^{sqr} and I_{ij}^{sqr}, the constraints are transformed from quadratic to linear [17]:

$$\begin{cases} -\alpha_{ij} M_1 \le P_{ij} \le \alpha_{ij} M_1, \\ -\alpha_{ij} M_2 \le Q_{ij} \le \alpha_{ij} M_2, \\ -\alpha_{ij} M_3 \le I_{ij} \le \alpha_{ij} M_3, \end{cases} \tag{12}$$

$$\begin{cases} \sum_{i\in f(j)} P_{ij} - r_{ij} I_{ij}^{sqr} = \sum_{k\in s(j)} P_{jk} + P_j, \\ \sum_{i\in f(j)} Q_{ij} - x_{ij} I_{ij}^{sqr} = \sum_{k\in s(j)} Q_{jk} + Q_j, \\ U_j^{sqr} = U_i^{sqr} - 2(r_{ij}P_{ij} + x_{ij}Q_{ij}) + (r_{ij}^2 + x_{ij}^2) I_{ij}^{sqr}, \\ U_i^{sqr} I_{ij}^{sqr} = P_{ij}^2 + Q_{ij}^2. \end{cases} \tag{13}$$

Here, M_1, M_2, and M_3 are sufficiently large positive numbers.

Further relaxation of the constraints in (13), which involve nonbranch disconnections, is achieved through the extended use of the Big M method:

$$\begin{cases} U_j^{sqr} \le M(1-\alpha_{ij}) + U_i^{sqr} - 2(r_{ij}P_{ij} + x_{ij}Q_{ij}) + (r_{ij}^2 + x_{ij}^2) I_{ij}^{sqr}, \\ U_j^{sqr} \ge -M(1-\alpha_{ij}) + U_i^{sqr} - 2(r_{ij}P_{ij} + x_{ij}Q_{ij}) + (r_{ij}^2 + x_{ij}^2) I_{ij}^{sqr}. \end{cases} \tag{14}$$

The relationship between voltage, current, and power in (13) of the constraints is nonlinear. To transform it, we employ second-order cone relaxation [18], [19]

$$\left\| \begin{matrix} 2P_{ij} \\ 2Q_{ij} \\ I_{ij}^{sqr} - U_i^{sqr} \end{matrix} \right\| \le I_{ij}^{sqr} + U_i^{sqr}. \tag{15}$$

C. Voltage and Current Constraints

Certain constraints must be applied to the node voltage and branch current after reconstruction:

$$\begin{cases} (U_i^{\min})^2 \le U_i^{sqr} \le (U_i^{\max})^2, \\ U_0^2 = 1, \\ 0 \le I_{ij}^{sqr} \le (I_{ij}^{\max})^2, \end{cases} \tag{16}$$

where $U_i^{\min}$ and $U_i^{\max}$ are the minimum and maximum allowable node voltage, U_0 is the balanced node voltage; $I_{ij}^{\max}$ is the maximum allowable current value.

D. Connectivity and Radiation Constraints

The connectivity and radiality of the distribution network need to be ensured after the reconstruction:

$$\begin{cases} \sum_{s\in s(j)} F_{js} - \sum_{s\in f(j)} F_{ij} = -1, j \in N \setminus N_{DG}, \\ -M\alpha_{ij} \le F_{ij} \le M\alpha_{ij}, \\ -M(2-\alpha_{ij}) \le F_{ij} \le M(2-\alpha_{ij}), \\ \sum_{ij\in\Omega_B} \alpha_{ij} = n-1, \end{cases} \tag{17}$$

where F_{js} and F_{ij}, respectively, represent the virtual power flow from node j to node s and from node i to node j, $f(j)$ is the child and parent of the node j, N_{DG} represents a collection of source nodes, n indicates the number of system nodes, and Ω_B is a collection of branches.

IV. RISK ASSESSMENT

This section will introduce the selection of evaluation indicators and the application of evaluation methods.

A. Risk Assessment Indicators

1. Voltage violation

The risk indicators for voltage violations include the probability of voltage violations and the severity of voltage violations.

The probability of voltage violation can be represented as [20]:

$$\begin{cases} P_v(\bar{V}_i) = P_v(V_i > V_{i\max}), \\ P_v(V_i) = P_v(V_i < V_{i\min}), \end{cases} \tag{18}$$

where the maximum allowable voltage in this paper is 1.05 and the minimum voltage is 0.95, $P_v(\bar{V}_i)$ is the probability of voltage exceeding the upper limit, and $P_v(V_i)$ is the probability of voltage falling below the lower limit.

Voltage violation severity:

$$\begin{cases} Sev(V_i) = \begin{cases} \dfrac{V_{\min} - V_i}{V_{\min}}, V_i < V_{\min}, \\ 0, V_i \ge V_{\min}, \end{cases} \\ Sev(\bar{V}_i) = \begin{cases} \dfrac{V_i - V_{\max}}{V_{\max}}, V_i > V_{\max}, \\ 0, V_i \le V_{\max}, \end{cases} \end{cases} \tag{19}$$

where $Sev(\bar{V}_i)$ is the severity of exceeding the upper limit and $Sev(V_i)$ is the severity of falling below the lower limit.

The risk indicators for voltage violation

$$R_v = \sum P_v(\bar{V}_i) Sev(\bar{V}) + \sum P_v(V_i) Sev(V). \tag{20}$$

2. Power flow violation

The risk indicators for branch power flow violation include the probability of active power flow violation and the severity of active power flow violation.

The probability of power flow violation:

$$P_s(S_{ij}) = P_s(S_{ij} > S_{ij,\max}). \tag{21}$$

Power flow violation severity

$$Sev(S_{ij}) = \begin{cases} \dfrac{S_{ij} - S_{ij,\max}}{S_{ij,\max}}, S_{ij} > S_{ij,\max}, \\ 0, S_{ij} \le S_{ij,\max}, \end{cases} \tag{22}$$

where $S_{ij,\max}$ is the upper bound of the active power flow allowed by the branch ij and $Sev(S_{ij})$ represents the risk value of power flow.

The risk value of branch power flow violation

$$R_s = \sum P_s(S_{ij}) Sev(S_{ij}). \tag{23}$$

3. Load shedding

When unable to reconfigure, introduce the concept of power circles with the DG node as the centre and the DG capacity as the radius to search. Convert as many loads as possible to island operation. Loads that cannot be converted to island operation are considered lost loads. Differentiate the importance of different loads using first, second, and third levels [21].

Load-shedding risk value

$$R_h = \frac{\sum_{n} \alpha_i P_i}{\sum_{m} \alpha_i P_i}, \tag{24}$$

where P_i represents the active power of node i, α_i represents the importance level of load i, n represents the number of nodes involved in load shedding, and m represents the total number of nodes.

B. Combination Weighting Method

1. Entropy weight method

This paper considers two scenarios: voltage violation and current flow violation, taking into account the indicators of violation probability and violation severity for each scenario. Since both indicators are negative indicators (lower values are better), they need to be normalised. Since both probability and severity are positive values, the normalisation process can be done directly by taking their reciprocals

$$x_{ij}(z) = \frac{1}{x_{ij}(z)}, \ (i = 1,...,n, \ j = 1,...,m), \tag{25}$$

where z represents different states. In this paper, the weight value of each state should be recalculated, so the weight obtained by the entropy weight method in each state is different. n represents the number of samples, and m represents the number of indicators.

Calculating the proportion of a sample value with respect to this indicator,

$$p_{ij}(z) = \frac{x_{ij}(z)}{\sum_{i=1}^{n} x_{ij}(z)}. \tag{26}$$

Calculating the entropy value of the indicator,

$$e_j(z) = -k \sum_{i=1}^{n} p_{ij}(z) \ln(p_{ij}(z)), \tag{27}$$

where $k = 1/\ln(n) > 0$.

Normalisation, the weights are obtained as follows

$$\omega_j(z) = \frac{1 - e_j(z)}{\sum_{j=1}^{m} 1 - e_j(z)}, \tag{28}$$

where ω_j represents the weights obtained after normalisation.

2. Analytic hierarchy process

The analytic hierarchy process (AHP) is a decision-making analysis method that establishes three levels of objectives, criteria, and alternatives, then conducts decision analysis based on a table of the scale system, and finally obtains subjective weights.

The general process of AHP is as follows. First, establish a hierarchical structure based on the problem, including the voltage, power flow, and loss of load, scheme level, and the indicator level of violation probability and severity. Second, establish a judgment matrix based on the scale system table. Then test the consistency of the judgment matrix and eliminate contradictions. Finally, normalise to obtain subjective weight values [22].

In this paper, the weight values for voltage violation, power flow overload, and loss of load obtained by AHP are fixed and unchanged.

3. Combination weighting and results

The method of combining subjective and objective weights can make the weights more reasonable. Assuming that a set of weights obtained by the subjective method is μ_j and a set of weights obtained by the objective method is $\omega_j(z)$, then the final weight

$$\lambda_j(z) = \frac{\mu_j \omega_j(z)}{\sum_{j=1}^{n} \mu_j \omega_j(z)}. \tag{29}$$

Multiply the risk value for a certain state by its corresponding probability and then sum up the results obtained for all states

$$Y = \sum_{z=1}^{t} P_g(z)(\lambda_1(z)R_v(z) + \lambda_2(z)R_s(z) + \lambda_3(z)R_h(z)), \tag{30}$$

where Y is the total risk value, $P_g(z)$ represents the probabilities of different states occurring, and t is the total number of states that occur.

C. Risk Assessment Process

The risk assessment process of this paper includes the following steps.

1. Input the basic parameters of the system, such as network nodes, branch resistance, reactance, expected values, and load variances.
2. Generate wind power, photovoltaic data, and load data using the Halton method based on the distributed stochastic model.
3. Generate samples of wind turbines, photovoltaics, and line states according to the component state model, record each state and its probability of occurrence.
4. Analyse each set of states, reconstruct states with line faults, and, for cases where reconstruction is not possible, first attempt islanding operation for loads and distributed power sources. If islanding operation is not feasible, cut off part of the load, resulting in a reconstructed or partially de-energised new distribution network structure.
5. Perform power flow calculation using distributed power output data and the reconstructed distribution network to

obtain node voltages, power flows, and loss of load conditions in each state. Assess the security of the distribution network through a combined weighting method.

V. SIMULATION ANALYSES

In this section, two case studies are analysed. The first is conducted on the standard IEEE33 bus system. The second case study is conducted on the IEEE118 bus system. The simulation analysis is carried out in the two above systems, and the rationality of applying this method to the risk assessment is verified.

A. IEEE33 Bus System

This simulation is built on the matlab2021b version. The parameter settings in this article are as follows. The two parameters for the Beta distribution of the photovoltaic model are set as 0.48 and 2.03, respectively. The photovoltaic conversion efficiency is set at 0.14. The two parameters for the wind power model are set to 6.2 and 2.7, respectively. The wind turbine cut-in wind speed is set to 3 m/s. The wind turbine cut-out wind speed is set as 11m/s. Wind turbine rated wind speed is set at 22 m/s. The topology of the IEEE33 bus system is shown in Fig. 1.

Consider the system states of no faults, single line faults, and two line faults. Wind power and solar power are connected to node 4 and node 6, with a capacity ranging from 200 kW to 800 kW. At this time, the connection point is at the front end of the system. Then wind power and solar power are connected to node 11 and node 14, with capacities ranging from 200 kW to 800 kW. At this time, the connection point is in the middle position of the system. Finally, wind power and solar power are both connected to node 17, with capacities ranging from 200 kW to 800 kW, and the connection point is at the end of the system.

As shown in Fig. 2, when the access point is located at the front end of the system, there is a downward trend, with lower and more stable risk values. As the access point moves to the end of the system, there is an upward trend, and both the position and the capacity of the access point have an impact on the system risk values. From simulation, it can be concluded that for distributed access distribution networks, access points with larger capacities should be connected to the front or middle positions of the system, whereas access points with smaller capacities should be connected to the rear positions of the system.

To analyse various states under multi-line faults, the rated power of 600 kW wind power and photovoltaic is connected to node 14.

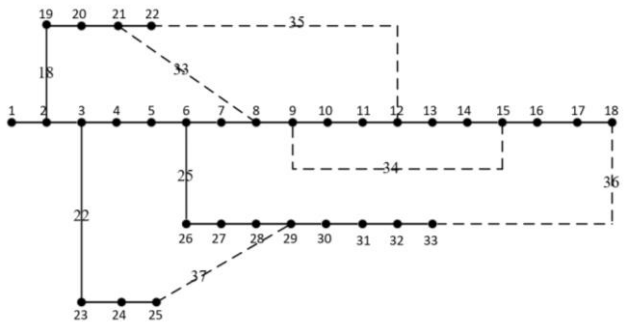

Fig. 1. Topology of the IEEE33 bus system.

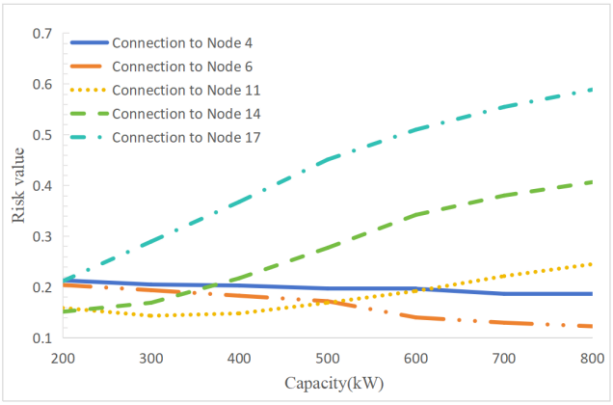

Fig. 2. IEEE33 multiline fault risk value.

There are approximately 80 randomly generated system states, 32 of which have a probability greater than 0.1 %. As can be seen from Table I, the system has the highest possibility of no fault line in the short term, and the probability of other line faults is only about 4 %. The probability of failure of wind turbines and photovoltaics is about 2.4 %. Single line fault is the main line fault state, the probability of double line fault state is low, and the influence on risk value is small. Figure 3 shows the average voltage of partial high probability states.

TABLE I. PARTIAL SYSTEM STATUS.

No.	Distribution State	Fault Location	Opened Branch	State Probability
1	0/1	\	\	0.52 %
2	1/0	\	\	1.76 %
3	1/1	\	\	93.9 %
4	1/1	4	4, 8, 27, 34, 36	0.15 %
5	1/1	9	9, 18, 24, 35, 36	0.15 %
6	1/1	6	6, 9, 15, 21, 26	0.14 %
7	1/1	14	14, 18, 21, 26, 34	0.14 %

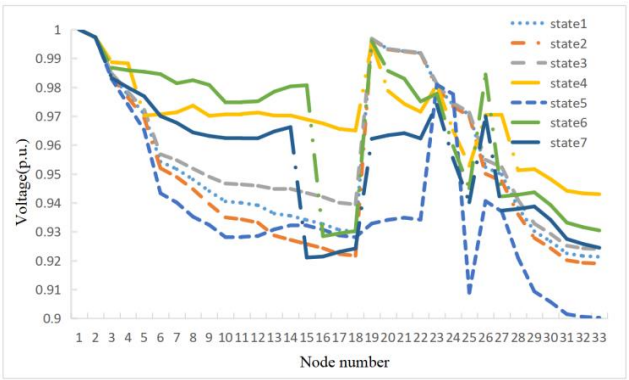

Fig. 3. Average voltage of partial high-probability states under multiline faults.

To verify the efficiency and accuracy of the Halton sequence method used, the Monte Carlo (MC) method is used as a comparison under the same parameters and evaluation indicator conditions. Wind turbines and photovoltaics with capacities ranging from 200 kW to 800 kW are connected to nodes 11, 14, and 17.

Table II shows a comparison of the risk values obtained by the two sampling methods. Compared to the MC method with 10000 sets of samples, the Halton sequence sampling method with 3000 sets of samples is used, and the time required for the case study is 50 % to 60 % of MC, with a maximum error of only 2 % compared to MC.

To validate the risk assessment method considering line

faults in this paper and compare it with the risk assessment under purely static conditions, the risk values obtained are compared under the same parameter selection, sampling method, and evaluation indicator method. Wind turbines and photovoltaics with capacities of 400 kW are connected at 10 important nodes: 4, 6, 10, 13, 15, 17, 20, 24, 28, and 30. Risk values are recorded and sorted in ascending order.

TABLE II. COMPARISON OF RISK VALUES FOR TWO SAMPLING METHODS.

Capacity/kW	connect to 11		connect to 14		connect to 17	
	MC	Halton	MC	Halton	MC	Halton
200	0.1556	0.1586	0.1486	0.1511	0.2131	0.2114
300	0.1426	0.1431	0.1695	0.1688	0.2932	0.2893
400	0.1462	0.1478	0.2203	0.2172	0.3702	0.3676
500	0.1703	0.1689	0.2791	0.277	0.4485	0.4508
600	0.1936	0.1918	0.3389	0.3419	0.5115	0.5097
700	0.2204	0.2213	0.3758	0.38	0.5547	0.5545
800	0.2452	0.2448	0.4025	0.4063	0.5862	0.5886

Table III shows that there is a difference in the risk values obtained when considering faults and when not considering faults. Near the beginning of the system, such as nodes 4 and 6, the risk values considering faults are lower than those not considering faults. At other locations, the risk values considering faults are slightly higher than those not considering faults. However, the difference in risk values obtained under the two conditions is not significant, mainly because the probability of normal operation in the short term is highest and the probability of faults occurring is relatively small.

TABLE III. COMPARISON OF RISK VALUES CONSIDERING FAULTS AND IGNORING FAULTS.

Location	Consider Fault		Ignore Fault	
	Risk value	sort	Risk value	sort
4	0.2027	7	0.2319	8
6	0.1826	5	0.215	6
10	0.1352	1	0.1293	1
13	0.1851	6	0.1813	5
15	0.2617	9	0.2558	9
17	0.3676	10	0.367	10
20	0.2219	8	0.2208	7
24	0.1704	4	0.1695	4
28	0.1452	2	0.138	2
30	0.1544	3	0.1453	3

Regardless of the situation considered, when the access points are closer to the middle of the system, such as nodes 10, 24, and 28, the risk values are lower; when closer to the beginning or end, such as nodes 4, 15, and 17, the risk values are higher. However, the method proposed in this paper considers the fault conditions and, combined with the use of combination weighting methods, makes the risk assessment of the distribution network more comprehensive and reasonable.

B. IEEE118 Bus System

The simulation is carried out on the IEEE118 bus system with unchanged parameter settings, and the topology is shown in Fig. 4.

The positions and capacities of photovoltaic and wind power access points are altered. Configuration points and capacities are shown in Table IV.

From Fig. 5, it can be seen that the results obtained from both the large-scale system and the small system are the same.

When access points are at the beginning, middle or near the front of the system, risk values are relatively low, and they show a decreasing trend with increasing capacity. However, the trend is not significant, indicating that the influence of capacity is small at this point.

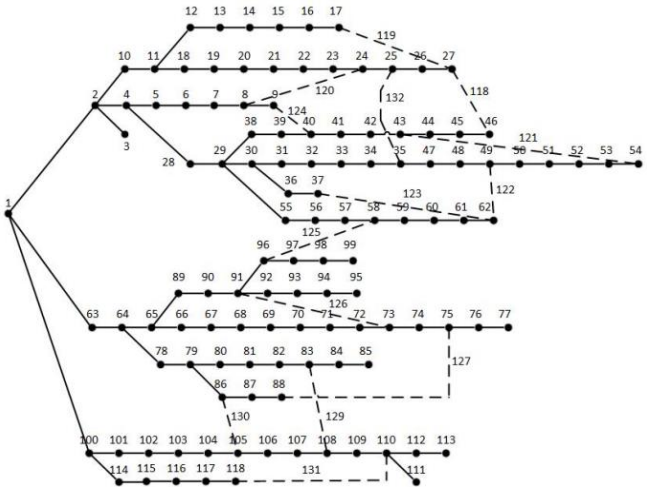

Fig. 4. Topology of the IEEE118 bus system.

TABLE IV. DISTRIBUTED POWER GENERATION ACCESS POINTS AND CAPACITIES.

Capacity/kW	Location					
	WT	PV	WT	PV	WT	PV
400	30	66	47	72	52	76
500	30	66	47	72	52	76
600	30	66	47	72	52	76
700	30	66	47	72	52	76
800	30	66	47	72	52	76
1000	30	66	47	72	52	76
1200	30	66	47	72	52	76
1400	30	66	47	72	52	76

When the access points are near the end of the system, the risk values increase significantly with increasing capacity. At the same time, it can also be observed that the risk values are low when the access points are in the middle of the system and high when they are near the beginning or end. Consistent conclusions are obtained for both the IEEE33 bus system and the IEEE118 bus system, validating the rationality of the method proposed in this paper.

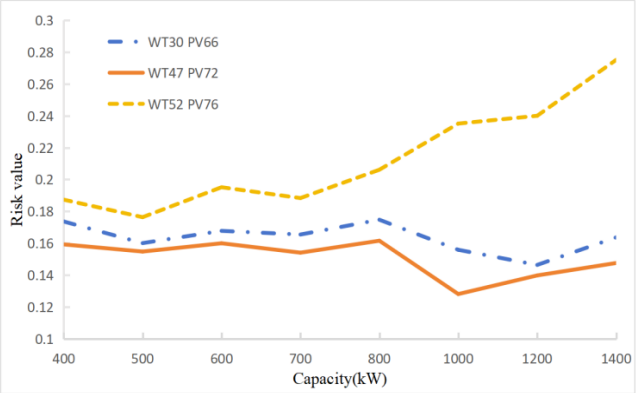

Fig. 5. IEEE118 multiline fault risk value.

VI. CONCLUSIONS

Regarding the issue of security risk assessment in distribution networks, this paper proposes a method for security risk assessment in distribution networks with distributed power sources, taking into account line reconfiguration. It simultaneously considers distributed power output, state uncertainty, and distribution line faults. Case studies have verified its effectiveness, and the conclusions are as follows:

1. The fault model of the distribution network component is established, the expected faults are generated, and the reconstructed model is used for the recovery of the fault, and the risk value is comprehensively calculated according to different fault situations. To analyse the influence of capacity and location of different distributed power supplies on the risk value, distributed power supplies should be connected to the middle and front of the system, and the access capacity should not be too large and can be dispersed into the system.
2. The Halton sequence method is used for sample sampling, which is more uniform than the Monte Carlo method. With the same results, the sample size can be reduced by 60 % to 70 %, thus reducing the calculation time by 60 % and improving the efficiency of distribution network risk assessment.
3. A large number of state samples are used to approximate the operating state and possible failure of the system. The product of the crossover risk value and the probability of occurrence of different indicators in various states of the expected accident is taken as the comprehensive risk value. This method can consider the safety and reliability of the distribution network at the same time, which is more reasonable than the traditional static distribution network risk assessment, which only analyses the risk value under normal operation.

CONFLICTS OF INTEREST

The authors declare that they have no conflicts of interest.

REFERENCES

[1] X. Wang, S. J. Yan, X. Y. Zhang, and K. J. Shi, "Risk assessment of photovoltaic distribution network based on probabilistic power flow with cumulant method", *Northeast Electric Power Technology*, vol. 43, no. 10, pp. 1–5, 2022. DOI: 10.3969/j.issn.1004-7913.2022.10.002.

[2] J. A. Zhang *et al*., "Distribution network risk assessment considering the flexible access of DG", *Distribution and Utilization*, vol. 36, no. 5, pp. 29–33, 2019. DOI: 10.19421/j.cnki.1006-6357.2019.05.005.

[3] W. Yan, Z. Ren, X. Zhao, J. Yu, Y. Li, and X. Hu, "Probabilistic photovoltaic power modeling based on nonparametric kernel density estimation", *Automation of Electric Power Systems*, vol. 37, no. 10, pp. 35–40, 2013. DOI: 10.7500/AEPS201203204.

[4] G. Ma, Y. N. Zhang, Z. Chen, Y. B. He, C. X. Guo, and J. J. Zhang, "Risk assessment method for hybrid AC/DC system with large-scale wind power integration", *Power System Technology*, vol. 43, no. 9, pp. 3241–3252, 2019. DOI: 10.13335/j.1000-3673.pst.2018.2348.

[5] Y. F. Ma, X. K. Yang, Z. J. Wang, L. Dong, S. Q. Zhao, and Y. Q. Cai, "Operation risk assessment for power system with large-scale wind power integration based on value at risk", *Power System Technology*, vol. 45, no. 3, pp. 849–855, 2021. DOI: 10.13335/j.1000-3673.pst.2020.0505.

[6] B. Che, Y. Z. Liu, R. Y. Yu, W. H. Yang, L. M. Ge, and X. Y. Wang, "Risk assessment method for distribution network considering the randomness of PV power", *Renewable Energy Resources*, vol. 37, no. 11, pp. 1685–1690, 2019. DOI: 10.13941/j.cnki.21-1469/tk.2019.11.017.

[7] X. Y. Kong, H. W. Li, D. Liu, and P. Zhang, "Research on safety assessment index system for new distribution networks", *Jiangxi Electric Power*, vol. 47, no. 1, pp. 35–37, 2023. DOI: 10.3969/j.issn.1006-348X.2023.01.009.

[8] R. X. Liu, J. H. Zhang, and D. Wu, "Research on static security index of distribution network based on risk theory", *Power System Protection and Control*, vol. 39, no. 15, pp. 89–95, 2011. DOI: 10.3969/j.issn.1674-3415.2011.15.018.

[9] X. Yu and Y. Xue, "Smart grids: A cyber-physical systems perspective", *Proceedings of the IEEE*, vol. 104, no. 5, pp. 1058–1070, 2016. DOI: 10.1109/JPROC.2015.2503119.

[10] R. T. He, X. Y. Zhang, H. Zhang, K. Huang, and R. Zhao, "Research on risk identification method of voltage stability of distribution network considering distributed energy", *Renewable Energy Resources*, vol. 38, no. 5, pp. 685–689, 2020. DOI: 10.13941/j.cnki.21-1469/tk.2020.05.019.

[11] X. P. Yang and L. J. Wang, "Optimization of distributed power distribution network based on probabilistic load flow", *Acta Energiae Solaris Sinica*, vol. 42, no. 8, pp. 71–76, 2021. DOI: 10.19912/j.0254-0096.tynxb.2019-0677.

[12] J. Le, J. F. Zhu, M. Sun, and W. Zeng, "Research on the risk assessment and countermeasures of distribution network with large scale distributed PV accessing", *Electrical Measurement & Instrumentation*, vol. 56, no. 14, pp. 28–33, 2019. DOI: 10.19753/j.issn1001-1390.2019.014.006.

[13] H. Y. Huang and W. J. Yu, "Power grid reliability assessment considering probability distribution of wind farm power output", *Power System Technology*, vol. 37, no. 9, pp. 2585–2591, 2013. DOI: 10.13335/j.1000-3673.pst.2013.09.038.

[14] H. Y. Shang, T. Q. Liu, T. Bu, C. He, Y. Yin, and L. J. Ding, "Operational risk assessment of power system considering wind power and photovoltaic grid connection", *Modern Electric Power*, vol. 37, no. 4, pp. 358–367, 2020. DOI: 10.19725/j.cnki.1007-2322.2020.0112.

[15] C. Li, Y. Zeng, C. Qin, Y. T. Song, and P. Ji, "Optimization method for power system dispatching considering operation risk", *Proceedings of the CSU-EPSA*, vol. 28, no. 6, pp. 73–79, 2016. DOI: 10.3969/j.issn.1003-8930.2016.06.013.

[16] B. Zhang, S. Y. Liu, Z. Z. Lin, L. Yang, and Q. Gao, "Distribution network reconfiguration with high penetration of renewable energy considering demand response and soft open point", *Automation of Electric Power Systems*, vol. 45, no. 8, pp. 86–94, 2021. DOI: 10.7500/AEPS20190930004.

[17] W. B. Hao, Z. G. Meng Y. Zhang, B. Xie, and P. Peng, "Carrying capacity evaluation of multiple distributed power supply access to the distribution network with the background of a new power system", *Power System Protection and Control*, vol. 51, no. 14, pp. 23–33, 2023. DOI: 10.19783/j.cnki.pspc.221534.

[18] Y. H. Wang, W. X. Liu, Q. Yao, H. Y. Wang, J. He, and X. J. Xiong, "Pre-layout and dynamic scheduling strategy of mobile energy storage for resilience enhancement of distribution network", *Automation of Electric Power Systems*, vol. 46, no. 15, pp. 37–45, 2022. DOI: 10.7500/AEPS20211228001.

[19] Y. S. Liang *et al*., "Real-time risk assessment and regulation strategy of new energy islanded distribution network based on probabilistic prediction and stochastic response surface methodology", *Power System Technology*, vol. 47, no. 12, pp. 4948–4961, 2023. DOI: 10.13335/j.1000-3673.pst.2023.1294.

[20] Z. Wang, C. H. Yang, J. Peng, T. T. Yang, and Y. L. Bai, "Research on adaptability for distributed PV generation connected to distribution network based risk evaluation with beyond limit", *Journal of Lanzhou University of Technology*, vol. 46, no. 4, pp. 91–95, 2020. DOI:

10.3969/j.issn.1673-5196.2020.04.017.

[21] F. Zhang *et al.*, "Study on island partition strategy of distribution network considering minimum load loss", *High Voltage Apparatus*, vol. 57, no. 4, pp. 181–188, 2021. DOI: 10.13296/j.1001-1609.hva.2021.04.026.

[22] Y. F. Ma, Z. R. Luo, S. Q. Zhao, Z. J. Wang, J. R. Xie, and S. M. Zeng, "Risk assessment of a power system containing wind power and photovoltaic based on improved Monte Carlo mixed sampling", *Power System Protection and Control*, vol. 50, no. 9, pp. 75–83, 2022. DOI: 10.19783/j.cnki.pspc.211076.

This article is an open access article distributed under the terms and conditions of the Creative Commons Attribution 4.0 (CC BY 4.0) license (http://creativecommons.org/licenses/by/4.0/).